Efficient energy preserving Galerkin–Legendre spectral methods for fractional nonlinear Schrödinger equation with wave operator

Dongdong Hu[1], Wenjun Cai[1], Xian-Ming Gu[2], Yushun Wang[1*]

[1]Jiangsu Key Laboratory for NSLSCS,

Jiangsu Collaborative Innovation Center of Biomedical Functional Materials,

School of Mathematical Sciences, Nanjing Normal University, Nanjing 210023, China

[2]School of Economic Mathematics/Institute of Mathematics,

Southwestern University of Finance and Economics, Chengdu, Sichuan 611130, China

Abstract

In this paper, we propose three energy preserving Galerkin–Legendre spectral methods, including the Crank–Nicolson Galerkin–Legendre spectral (CN–GLS) method, the energy quadratization Galerkin-Legendre spectral method based on scalar auxiliary variable approach (SAV–GLS), and the linearly implicit Galerkin–Legendre spectral method based on exponential scalar auxiliary variable approach (ESAV–GLS), for the space fractional nonlinear Schrödinger equation with wave operator. In theoretical analyses, we take the CN–GLS method as an example to analyze the associate $L^{\infty}-$norm boundness and the unconditional spectral-accuracy convergence in L^{∞} norm. The effective numerical implementations of the proposed spectral Galerkin methods are discussed in detail. Extensive numerical comparisons illustrate that the theoretical results are correct and the proposed spectral Galerkin methods have high efficiency for energy preserving in long–time computations.

AMS subject classification: 26A33, 70H0, 65M125, 65N35

Keywords: Fractional nonlinear Schrödinger equation; Galerkin–Legendre spectral method; Conservative scheme; Maximum norm error estimate; Stability; Spectral-accuracy convergence

1 Introduction

We consider the development of numerical methods for the following fractional cubic nonlinear Schrödinger (FNLS) equation with wave operator in the bounded domain $\Omega = (a, b)$, i.e.,

$$u_{tt} + (-\Delta)^{\frac{\alpha}{2}} u + \mathrm{i}\kappa u_t + \beta |u|^2 u = 0 \quad \text{in} \quad \Omega \times (0, T], \tag{1.1}$$

$$u(x, 0) = u_0(x), \quad u_t(x, 0) = u_1(x) \quad \text{in} \quad \Omega, \tag{1.2}$$

$$u(x, t) = 0 \quad \text{on} \quad \partial\Omega \times (0, T]. \tag{1.3}$$

where $u(x, t)$ is a complex function, $1 < \alpha < 2$, κ and β are positive real constants, $u_0(x)$ and $u_1(x)$ are given smooth functions, and $\mathrm{i}^2 = -1$. The fractional Laplacian is defined with Cauchy principle value, i.e.

$$-(-\Delta)^{\frac{\alpha}{2}} u(x) = -c_\alpha \mathrm{P.V.} \int_\Omega \frac{u(x) - u(y)}{|x - y|^{1+\alpha}} dy, \quad c_\alpha = \frac{2^\alpha \Gamma(\frac{\alpha+1}{2})}{\pi^{1/2} |\Gamma(-\alpha/2)|},$$

*Correspondence author. Email addresses: hudongdong2021@gmail.com (Dongdong Hu), caiwenjun@njnu.edu.cn (Wenjun Cai), guxm@swufe.edu.cn (Xian-Ming Gu), wangyushun@njnu.edu.cn (Yushun Wang).

which is also equivalent to the Riesz fractional derivative [29]

$$-(-\Delta)^{\frac{\alpha}{2}}u = \frac{\partial^{\alpha}}{\partial|x|^{\alpha}}u = -\frac{1}{2\cos(\frac{\alpha\pi}{2})}\left[{}^{RL}_{a}D^{\alpha}_{x} + {}^{RL}_{x}D^{\alpha}_{b}\right]u,$$

where the left and right Riemann-Liouville fractional derivatives are defined as

$${}^{RL}_{a}D^{\alpha}_{x}u = \frac{1}{\Gamma(2-\alpha)}\frac{\partial^2}{\partial x^2}\int_a^x \frac{u(\xi,t)d\xi}{(x-\xi)^{\alpha-1}}, \quad {}^{RL}_{x}D^{\alpha}_{b}u = \frac{1}{\Gamma(2-\alpha)}\frac{\partial^2}{\partial x^2}\int_x^b \frac{u(\xi,t)d\xi}{(\xi-x)^{\alpha-1}},$$

in which $\Gamma(z) = \int_0^{\infty} x^{z-1}e^{-x}dx$.

It is well known that the solutions of FNLS equation (1.1) conserves the total energy

$$\mathcal{E}(t) = \int_{\Omega}(u_t)^2 + \bar{u}(-\Delta)^{\frac{\alpha}{2}}u + \frac{\beta}{2}|u|^4 dx = \mathcal{E}(0),$$

where $\bar{u}$ is the complex conjugate of u.

The nonlinear Schrödinger (NLS) equation is famous for that it has been widely applied in many fields of physics, involving quantum physics, plasma physics and nonlinear optics [26, 33, 43]. It is derived by using Feynman path integrals over Brownian process. Recently, Laskin [25] confirms that the Lévy-like process offers possibilities for us to develop the fractional quantum mechanics which is a generalized quantum mechanics. In virtue of such an attempt, the fractional nonlinear Schrödinger equation is proposed, which including the fractional Laplacian with the Lévy index α instead of the classical one. While for $\alpha = 2$, the FNLS equation reduces to the classical cubic NLS equation, In the special case of $\beta = 0$, it collapses to the fractional nonlinear wave equation [24, 31]. Nowadays, the FNLS equation has drawn much attention in propagation dynamics [47], water wave dynamics [22] and biopolymers [23]. Other studies on the Cauchy problem, the existence of solitary wave solutions of the FNLS equation (1.1) have been studied, readers can refer [3, 6, 13, 14] for more details.

Indeed, it is hard for researchers to discuss the analytical solution for the FNLS equation due to the nonlocality of the fractional Laplacian and nonlinearity of the fractional model. Designing efficient numerical methods for the model (1.1) is important for us to recognize the solitary wave propagation of the FNLS equation. Moreover, the key of the numerical method is the approximation of fractional Laplacian. In recent years, there are a large amount of literature on numerical approaches and numerical analyses of the fractional Laplacian, such as the finite difference methods [9, 10, 16, 19, 20, 39, 45], finite element methods [4, 41] and spectral methods [38, 46] and so on. While for the FNLS equation (1.1), there exist some works on numerical methods, for example, we refer readers to finite difference method [34, 35] and finite element method [8, 27] and references therein.

Numerous theoretical and experimental results indicate that the structure preserving algorithms can preserve the intrinsic physical invariants of the nonlinear conservative systems and often have excellent numerical properties, such as the linear error growth, long-time behavior and smaller amplitude [18]. One of the most important component of the structure preserving scheme is exactly the time-stepping approach. The well-know invariant-preserving integrators for conservative systems are about the averaged vector field (AVF) methods [32], the discrete variational derivative (DVD) methods [12] and the Hamiltonian boundary value methods (HBVMs) [5] and so on.

The objective of this paper is to develop the energy preserving numerical schemes with spectral accuracy for FNLS equation (1.1). After the spatial approximation by the Galerkin-Legendre spectral method for the FNLS equation, we first present the Crank-Nicolson energy preserving spectral Galerkin method. Second, we construct the energy quadratization energy preserving spectral Galerkin method by using the SAV approach [37]. Third, we propose the linearly implicit energy preserving spectral Galerkin method by utilizing the ESAV approach [28]. The other significance of this paper is that we establish the spectral-accuracy convergence and stability in L^2 and L^∞ norm without grid-ratio condition for the CN–GLS method. Extensive numerical results demonstrate that the proposed spectral Galerkin-Legendre methods perform more effective than the comparing numerical schemes in numerical accuracy and energy preserving.

The rest of this paper is organized as follows. In Section 2, we introduce some fractional Sobolev spaces and lemmas. In Section 3, we construct the CN–GLS method and discuss the associated theoretical analyses. Then, we establish the SAV–GLS method and ESAV–GLS method in Section 4 and Section 5, respectively. In Section 6, we give the brief implementation to illustrate the numerical schemes. Finally, we report some numerical results for comparisons in Section 7 and draw some conclusions in Section 8.

2 Preliminaries

In this section, we introduce some essential definitions and lemmas of the spectral Galerkin method.

Definition 2.1 ([27]). *Define the inner product, L^p-norm $(1 \le p < \infty)$ and L^∞-norm as*

$$(u,v) = \int_\Omega \bar{v} u dx, \quad \|u\| = \sqrt{(u,u)}, \quad \|u\|_p := (\int_\Omega |u|^p dx)^{1/p}, \quad \|u\|_\infty := \operatorname{ess}\sup_{x\in\Omega}\{|u(x)|\},$$

Definition 2.2 (**Left fractional derivative space** [11, 46]). *For $\mu > 0$, define the semi-norms and norms of the left, right and symmetric fractional derivative spaces on Ω as*

$$|u|_{J_L^\mu(\Omega)} := \left(\|{}_a^{RL}D_x^\mu u\|^2 + \|{}_c^{RL}D_y^\mu u\|^2\right)^{1/2}, \quad \|u\|_{J_L^\mu(\Omega)} := \left(\|u\|^2 + |u|^2_{J_L^\mu(\Omega)}\right)^{1/2}.$$

$J_L^\mu(\Omega)$ (or $J_{L,0}^\mu(\Omega)$) denotes the closure of $C^\infty(\Omega)$ (or $C_0^\infty(\Omega)$) with respect to $\|\cdot\|_{J_L^\mu(\Omega)}$.

Definition 2.3 (**Right fractional derivative space** [11, 46]). *For $\mu > 0$, define the semi-norm and the norm as*

$$|u|_{J_R^\mu(\Omega)} := \left(\|{}_x^{RL}D_b^\mu u\|^2 + \|{}_x^{RL}D_d^\mu u\|^2\right)^{1/2}, \quad \|u\|_{J_R^\mu(\Omega)} := \left(\|u\|^2 + |u|^2_{J_R^\mu(\Omega)}\right)^{1/2}.$$

$J_R^\mu(\Omega)$ (or $J_{R,0}^\mu(\Omega)$) denotes the closure of $C^\infty(\Omega)$ (or $C_0^\infty(\Omega)$) with respect to $\|\cdot\|_{J_R^\mu(\Omega)}$.

Definition 2.4 (**Symmetric fractional derivative space** [11, 46]). *For $\mu > 0$, where $\mu \neq n - 1/2, n \in \mathbb{N}$, define the semi-norm and the norm as*

$$|u|_{J_S^\mu(\Omega)} := \left(|({}_a^{RL}D_x^\mu u, {}_x^{RL}D_b^\mu u)| + |({}_c^{RL}D_y^\mu u, {}_y^{RL}D_d^\mu u)|\right)^{1/2}, \quad \|u\|_{J_S^\mu(\Omega)} := \left(\|u\|^2 + |u|^2_{J_S^\mu(\Omega)}\right)^{1/2}.$$

$J_S^\mu(\Omega)$ (or $J_{S,0}^\mu(\Omega)$) denotes the closure of $C^\infty(\Omega)$ (or $C_0^\infty(\Omega)$) with respect to $\|\cdot\|_{J_S^\mu(\Omega)}$.

Definition 2.5 (**Fractional Sobolev space** [11, 46]). *For $\mu > 0$, define the semi-norm and the norm as*

$$|u|_{H^\mu(\Omega)} := \||\xi|^\mu \mathcal{F}[u,\xi]\|, \quad \|u\|_{H^\mu(\Omega)} := \left(\|u\|^2 + |u|^2_{H^\mu(\Omega)}\right)^{1/2}.$$

$H^\mu(\Omega)$ (or $H_0^\mu(\Omega)$) denotes the closure of $C^\infty(\Omega)$ (or $C_0^\infty(\Omega)$) with respect to $\|\cdot\|_{H^\mu(\Omega)}$.

Lemma 2.1 ([11, 46]). *Suppose $\mu > 0$ and $\mu \neq n - 1/2, n \in \mathbb{N}$. Then the spaces $J_L^\mu(\Omega)$, $J_R^\mu(\Omega)$, $J_S^\mu(\Omega)$ and $H^\mu(\Omega)$ are equal with equivalent seminorms and norms, and the spaces $J_{L,0}^\mu(\Omega)$, $J_{R,0}^\mu(\Omega)$, $J_{S,0}^\mu(\Omega)$ and $H_0^\mu(\Omega)$ are equal with equivalent seminorms and norms.*

Lemma 2.2 ([11, 46]). *Suppose $1 < \mu \le 2$. For any $u \in H_0^\mu(\Omega)$ and $v \in H_0^{\mu/2}(\Omega)$, we have*

$$({}_a^{RL}D_x^\mu u, v) = ({}_a^{RL}D_x^{\mu/2} u, {}_x^{RL}D_b^{\mu/2} v), \quad ({}_x^{RL}D_b^\mu u, v) = ({}_x^{RL}D_b^{\mu/2} u, {}_a^{RL}D_x^{\mu/2} v).$$

Lemma 2.3 (**Fractional Poincaré-Friedrichs inequality** [11, 46]). *For $u \in J^{\mu}_{L,0}(\Omega)$ and $0 < \lambda \le \mu$, it holds that*

$$\|u\| \le \mathcal{C}|u|_{J^{\mu}_{L}(\Omega)}, \quad \|u\|_{J^{\lambda}_{L}(\Omega)} \le \mathcal{C}|u|_{J^{\mu}_{L}(\Omega)}.$$

Besides, for $u \in J^{\mu}_{R,0}(\Omega)$ and $0 < \lambda \le \mu$, we have

$$\|u\| \le \mathcal{C}|u|_{J^{\mu}_{R}(\Omega)}, \quad \|u\|_{J^{\lambda}_{R}(\Omega)} \le \mathcal{C}|u|_{J^{\mu}_{R}(\Omega)}.$$

Similar conclusion can be deduced for $u \in H^{\mu}_{0}(\Omega)$ and $\mu \ne n - 1/2, n \in \mathbb{N}$.

3 Crank–Nicolson Galerkin–Legendre spectral method

Define the following bilinear form

$$\mathcal{A}(u,w) = \frac{1}{2\cos(\frac{\alpha\pi}{2})}\Big(({}^{RL}_{a}D^{\alpha/2}_{x}u, {}^{RL}_{x}D^{\alpha/2}_{b}w) + ({}^{RL}_{x}D^{\alpha/2}_{b}u, {}^{RL}_{a}D^{\alpha/2}_{x}w)\Big) \quad \forall u, w \in H^{\alpha/2}_{0}(\Omega).$$

For simplicity, we introduce the seminorm and the norm as

$$|u|_{\alpha/2} := \sqrt{\mathcal{A}(u,u)}, \quad \|u\|_{\alpha/2} := (\|u\|^2 + |u|^2_{\alpha/2})^{1/2}.$$

The bilinear form $\mathcal{A}(u,w)$ has the continuous and coercive properties [11], i.e., there exist positive constants C_1 and C_2, for any $u, w \in H^{\alpha/2}_{0}(\Omega)$, such that

$$|\mathcal{A}(u,w)| \le C_1\|u\|_{\alpha/2}\|v\|_{\alpha/2}, \quad |\mathcal{A}(u,u)| \ge C_2\|u\|^2_{\alpha/2}.$$

Based on Lemma 2.4 and the definition of Riesz fractional derivative, the weak formulation of (1.1) reads: finding $u \in H^{\alpha/2}_{0}(\Omega)$, such that

$$\mathrm{i}\kappa(u_t, w) + (u_{tt}, w) + \mathcal{A}(u,w) + \beta(|u|^2u, w) = 0, \quad \forall w \in H^{\alpha/2}_{0}(\Omega), \tag{3.1}$$

with the initial conditions given by

$$u(x,0) = u_0, \quad u_t(x,0) = u_1(x).$$

3.1 The CN-GLS method

Introduce $v = u_t$ to reformulate (3.1). Finding $u, v \in H^{\alpha/2}_{0}(\Omega)$, for $w \in H^{\alpha/2}_{0}(\Omega)$, such that

$$\begin{aligned}
&(u_t, w) = (v, w),\\
&(v_t, w) + \mathcal{A}(u,w) + \mathrm{i}\kappa(v,w) + \beta(|u|^2u, w) = 0,
\end{aligned}$$

For simplicity, we introduce the following notations for $n = 0, 1, \cdots, N_t$,

$$u^n = u(x,t_n), \quad \delta_t u^{n+\frac{1}{2}} = \frac{u^{n+1} - u^n}{\tau}, \quad u^{n+\frac{1}{2}} = \frac{u^{n+1} + u^n}{2}, \quad \widetilde{u}^{n+\frac{1}{2}} = \frac{3u^n - u^{n-1}}{2},$$

where $t_n = n\tau$, and $\tau = T/N_t$ is the time step size. We denote u^n and U^n_N is the exact solution and numerical approximation at $t = t_n$, respectively. For theoretical, we assume that $\max\limits_{0\le t\le T}\{\|u\|_\infty\} \le \mathcal{C}$. Without loss of generality, let $\mathcal{C}$ be a general positive constant which are independent of τ and N. For a fixed positive integer N, denote $P_N(\Omega)$ to be the space of polynomials with the degree no more than N on the interval $\Omega = (a,b)$. The approximation space X^0_N is defined as

$$X^0_N(\Omega) = P_N(\Omega) \cap H^{\alpha/2}_{0}(\Omega).$$

It is clear that $X_N^0(\Omega)$ is a subspace of $H_0^{\alpha/2}(\Omega)$. By using the modified Crank-Nicolson scheme for temporal derivative in (3.1), the Crank-Nicolson scheme with truncation errors reads: finding $u^n, v^n \in H_0^{\alpha/2}(\Omega)$, for $w \in H_0^{\alpha/2}(\Omega)$, such that

$$(\delta_t u^{n+\frac{1}{2}}, w) = (v^{n+\frac{1}{2}}, w) + (\mathcal{R}_1^{n+\frac{1}{2}}, w), \tag{3.2}$$

$$(\delta_t v^{n+\frac{1}{2}}, w) + \mathcal{A}(u^{n+\frac{1}{2}}, w) + \mathrm{i}\kappa(v^{n+\frac{1}{2}}, w) + \frac{\beta}{2}\Big((|u^n|^2 + |u^{n+1}|^2)u^{n+\frac{1}{2}}, w\Big) = (\mathcal{R}_2^{n+\frac{1}{2}}, w). \tag{3.3}$$

By eliminating error terms, the associated fully discrete CN–GLS scheme reads: finding $U_N^n, V_N^n \in X_N^0(\Omega)$, for $w_N \in X_N^0(\Omega)$, such that

$$(\delta_t U_N^{n+\frac{1}{2}}, w_N) = (V_N^{n+\frac{1}{2}}, w_N), \tag{3.4}$$

$$(\delta_t V_N^{n+\frac{1}{2}}, w_N) + \mathcal{A}(U_N^{n+\frac{1}{2}}, w_N) + \mathrm{i}\kappa(V_N^{n+\frac{1}{2}}, w_N) + \frac{\beta}{2}\Big((|U_N^n|^2 + |U_N^{n+1}|^2)U_N^{n+\frac{1}{2}}, w_N\Big) = 0, \tag{3.5}$$

with the initial conditions

$$U_N^0 = \Pi_N^{\alpha/2,0} u_0, \quad V_N^0 = \Pi_N^{\alpha/2,0} u_1,$$

where the orthogonal projection operator $\Pi_N^{\alpha/2,0}u$: $H_0^{\alpha/2}(\Omega) \to X_N^0$ is defined as

$$\mathcal{A}(u - \Pi_N^{\alpha/2,0}u, w_N) = 0, \quad \forall w_N \in X_N^0.$$

The orthogonal projection operator $\Pi_N^{\alpha/2,0}$ has the following properties.

Lemma 3.1 ([46])**.** *Let μ and r be arbitrary real numbers satisfying $\frac{1}{2} < \mu \leq 1 < r$. Then there exists a positive constant $\mathcal{C}$ independent of N, such that, for any function $u \in H^r(\Omega) \cap H_0^{\mu}(\Omega)$, the following estimate holds:*

$$\|u - \Pi_N^{\mu,0}u\| \leq \mathcal{C}N^{-r}\|u\|_{H^r(\Omega)},$$
$$|u - \Pi_N^{\mu,0}u|_\mu \leq \mathcal{C}N^{\mu-r}\|u\|_{H^r(\Omega)}.$$

Theorem 3.1 (**CN–GLS: Conservative law**)**.** *The numerical solution of the CN–GLS scheme (3.4)-(3.5) is conservative in the sense that*

$$\mathcal{E}^{n+1} = \mathcal{E}^n = \cdots = \mathcal{E}^0,$$

with

$$\mathcal{E}^n = \|V_N^n\|^2 + |U_N^n|^2_{\alpha/2} + \frac{\beta}{2}\|U_N^n\|_4^4, \quad 0 \leq n \leq N_t.$$

Proof. Choosing $w_N = \delta_t U_N^{n+\frac{1}{2}}$ in (3.5), and taking the real part to arrive at

$$\mathrm{Re}\Big\{(\delta_t V_N^{n+\frac{1}{2}}, \delta_t U_N^{n+\frac{1}{2}}) + \mathcal{A}(U_N^{n+\frac{1}{2}}, \delta_t U_N^{n+\frac{1}{2}}) + \frac{\beta}{2}\Big((|U_N^n|^2 + |U_N^{n+1}|^2)U_N^{n+\frac{1}{2}}, \delta_t U_N^{n+\frac{1}{2}}\Big)\Big\} = 0, \tag{3.6}$$

where "Re" represents the real part of a complex number.

In view of

$$\mathrm{Re}(\delta_t V_N^{n+\frac{1}{2}}, \delta_t U_N^{n+\frac{1}{2}}) = \mathrm{Re}(\delta_t V_N^{n+\frac{1}{2}}, V_N^{n+\frac{1}{2}}) = \frac{\|V_N^{n+1}\|^2 - \|V_N^n\|^2}{2\tau}, \tag{3.7}$$

$$\mathrm{Re}\Big\{\mathcal{A}(U_N^{n+\frac{1}{2}}, \delta_t U_N^{n+\frac{1}{2}})\Big\} = \frac{|U_N^{n+1}|^2_{\alpha/2} - |U_N^n|^2_{\alpha/2}}{2\tau}, \tag{3.8}$$

and

$$\mathrm{Re}\Big((|U_N^n|^2+|U_N^{n+1}|^2)U_N^{n+\frac{1}{2}},\delta_t U_N^{n+\frac{1}{2}}\Big)=\frac{\|U_N^{n+1}\|_4^4-\|U_N^n\|_4^4}{2\tau}. \tag{3.9}$$

Substituting (3.7)-(3.9) into (3.6), we obtain

$$\|V_N^{n+1}\|^2+|U_N^{n+1}|_{\alpha/2}^2+\frac{\beta}{2}\|U_N^{n+1}\|_4^4=\|V_N^n\|^2+|U_N^n|_{\alpha/2}^2+\frac{\beta}{2}\|U_N^n\|_4^4.$$

This ends the proof. □

3.2 The prior bound

Lemma 3.2 (**Gronwall inequality** [44]). *Suppose that the discrete grid function $\{w^n \mid n=0,1,2,\cdots,N_t;\ N_t\tau=T\}$ satisfies the following inequality*

$$w^n-w^{n-1}\le A\tau w^n+B\tau w^{n-1}+C_n\tau,$$

where A, B and C_n are non-negative constants, then

$$\max_{1\le n\le N_t}|w^n|\le\Big(w^0+\tau\sum_{k=1}^{N_t}C_k\Big)e^{2(A+B)T},$$

where τ is sufficiently small, such that $(A+B)\tau\le\frac{N_t-1}{2N_t}<\frac{1}{2}$, $(N_t>1)$.

Lemma 3.3 (**Sololev inequality** [23]). *For $\frac{1}{2}<\mu\le 1$, then there exists a positive constant $\mathcal{C}$, such that*

$$\|u\|_\infty\le\mathcal{C}\|u\|_{H^\mu},\quad \forall u\in H_0^\mu(\Omega).$$

Theorem 3.2. *The numerical solution of the scheme (3.4)-(3.5) is long-time bounded in the following sense*

$$\|U_N^n\|\le\mathcal{C},\quad \|V_N^n\|\le\mathcal{C},\quad |U_N^n|_{\alpha/2}\le\mathcal{C},\quad \|U_N^n\|_\infty\le\mathcal{C},\quad 0\le n\le N_t.$$

Proof. According to Theorem 3.1, we derive

$$\|V_N^n\|+|U_N^n|_{\alpha/2}\le\mathcal{C},$$

whihc implies

$$\max_{1\le n\le N_t}\Big\{\|V_N^n\|,|U_N^n|_{\alpha/2}\Big\}\le\mathcal{C}.$$

In virtue of (3.4) and the Grownwall inequality (Lemma 3.2), for sufficient small τ, we deduce

$$\|U_N^{n+1}\|\le\|U_N^n\|+\frac{\tau}{2}(\|V_N^{n+1}\|+\|V_N^n\|)\le\mathcal{C}.$$

In view of the Sololev inequality (Lemma 3.3), we have

$$\|U_N^n\|_\infty\le\mathcal{C}\sqrt{\|U_N^n\|+|U_N^n|_{\alpha/2}}\le\mathcal{C}.$$

This ends the proof. □

3.3 Solvability

Theorem 3.3. *The solution of difference scheme (3.4)-(3.5) uniquely exists.*

Proof. Browder fixed point theorem [1] is applied to show the unique solvability. Indeed, the proof is very similar as Ref. [40] by combining Lemma 3.2. Here we omit the proof for brevity. □

3.4 Stability and convergence analysis for the CN–GLS method

Lemma 3.4. *Suppose that the exact solution $u(\cdot,t) \in C^3([0,T])$. Then we have*

$$\max_{0\le n\le N_t-1}\left\{\|\mathcal{R}_1^{n+1/2}\|, \|\mathcal{R}_2^{n+1/2}\|\right\} \le \mathcal{C}\tau^2.$$

where $\mathcal{C}$ is a positive constant independent of N and τ.

Proof. The proof can be obtained by Taylor's expansion. Similar procedures, please refer to Refs. [21, 40]. ☐

Theorem 3.4. *Suppose $u \in C^3(0,T;H^r(\Omega)\cap H_0^{\alpha/2}(\Omega))$ $(r>1)$ is the solution of (1.1) and U_N^n is the solution of (3.4)-(3.5), respectively. For sufficiently small step τ and N^{-1}, the CN–GLS scheme is convergent in the sense that*

$$\|u^n - U_N^n\| \le \mathcal{C}(\tau^2 + N^{\alpha/2-r}), \qquad \|u^n - U_N^n\|_\infty \le \mathcal{C}(\tau^2 + N^{\alpha/2-r}), \quad 1\le n\le N_t.$$

Proof. Denote the errors function

$$\begin{aligned}
\varepsilon_u^n &= u^n - U_N^n = (u^n - \Pi_N^{\alpha/2,0}u^n) + (\Pi_N^{\alpha/2,0}u^n - U_N^n) = \eta_u^n + \xi_u^n,\\
\varepsilon_v^n &= v^n - V_N^n = (v^n - \Pi_N^{\alpha/2,0}v^n) + (\Pi_N^{\alpha/2,0}v^n - V_N^n) = \eta_v^n + \xi_v^n,\\
\varepsilon_u^0 &= u_0 - \Pi_N^{\alpha/2,0}u_0, \qquad \varepsilon_v^0 = u_1 - \Pi_N^{\alpha/2,0}u_1.
\end{aligned}$$

In view of the definition of orthogonal projection operator $\Pi_N^{\alpha/2,0}$, the consequence holds

$$(\eta_u^n, w_N) = 0, \quad (\eta_v^n, w_N) = 0, \quad \forall w_N \in X_N^0.$$

Subtracting (3.4)-(3.5) from (3.2)-(3.3), for $w_N \in X_N^0(\Omega)$, we obtain the error equations

$$(\delta_t \xi_u^{n+\frac12}, w_N) = (\xi_v^{n+\frac12}, w_N) + (\mathcal{R}_1^{n+\frac12}, w_N), \tag{3.10}$$

$$(\delta_t \xi_v^{n+\frac12}, w_N) + \mathcal{A}(\xi_u^{n+\frac12}, w_N) + \mathrm{i}\kappa(\xi_v^{n+\frac12}, w_N) + \frac{\beta}{2}\Big(\mathcal{N}^{n+1/2}, w_N\Big) = (\mathcal{R}_2^{n+\frac12}, w_N), \tag{3.11}$$

in which

$$\begin{aligned}
\mathcal{N}^{n+1/2} &= (|u^n|^2 + |u^{n+1}|^2)u^{n+\frac12} - (|U_N^n|^2 + |U_N^{n+1}|^2)U_N^{n+\frac12}\\
&= (|U_N^n|^2 + |U_N^{n+1}|^2)\varepsilon_u^{n+\frac12} + \Big[(|u^n|^2 + |u^{n+1}|^2) - (|U_N^n|^2 + |U_N^{n+1}|^2)\Big]u^{n+\frac12}\\
&= \mathcal{N}_1^{n+1/2} + \mathcal{N}_1^{n+1/2}.
\end{aligned} \tag{3.12}$$

Based on Theorem 3.1, Lemma 3.2 and the assumption on exact solution, we deduce

$$\|\mathcal{N}_1^{n+1/2}\|^2 = \Big\|(|U_N^n|^2 + |U_N^{n+1}|^2)\varepsilon_u^{n+\frac12}\Big\|^2 \le \mathcal{C}(\|\varepsilon_u^{n+1}\|^2 + \|\varepsilon_u^n\|^2), \tag{3.13}$$

and

$$\begin{aligned}
\|\mathcal{N}_2^{n+1/2}\|^2 = &\Big\|\Big[2\mathrm{Re}(\bar{\varepsilon}_u^{n+1}u^{n+1}) - \bar{\varepsilon}_u^{n+1}(u^{n+1} - U_N^{n+1}) + 2\mathrm{Re}(\bar{\varepsilon}_u^{n}u^{n}) - \bar{\varepsilon}_u^{n}(u^{n} - U_N^{n})\Big]u^{n+\frac12}\Big\|^2\\
&\le \mathcal{C}(\|\varepsilon_u^{n+1}\|^2 + \|\varepsilon_u^n\|^2).
\end{aligned} \tag{3.14}$$

Therefore, we have

$$\|\mathcal{N}^{n+1/2}\|^2 \le \mathcal{C}(\|\mathcal{N}_1^{n+1/2}\|^2 + \|\mathcal{N}_2^{n+1/2}\|^2) \le \mathcal{C}(\|\varepsilon_u^{n+1}\|^2 + \|\varepsilon_u^n\|^2) \le \mathcal{C}(\|\xi_u^{n+1}\|^2 + \|\xi_u^n\|^2 + N^{-2r}), \tag{3.15}$$

where Lemma 3.1 is used in the last inequality.

Choosing $w_N = \xi_u^{n+1/2}$ in (3.10) and taking the real part, by using the Cauchy-Schwarz inequality, we get

$$\begin{aligned}\frac{\|\xi_u^{n+1}\|^2 - \|\xi_u^n\|^2}{2\tau} &= \mathrm{Re}\Big\{(\xi_v^{n+\frac{1}{2}}, \xi_u^{n+1/2}) + (\mathcal{R}_1^{n+\frac{1}{2}}, \xi_u^{n+1/2})\Big\} \\ &\leq \mathcal{C}(\|\xi_u^{n+1}\|^2 + \|\xi_u^n\|^2 + \|\xi_v^{n+1}\|^2 + \|\xi_v^n\|^2 + \tau^4),\end{aligned} \tag{3.16}$$

and thus,

$$\|\xi_u^{n+1}\|^2 \leq \|\xi_u^n\|^2 + \mathcal{C}\tau(\|\xi_u^{n+1}\|^2 + \|\xi_u^n\|^2 + \|\xi_v^{n+1}\|^2 + \|\xi_v^n\|^2 + \tau^4). \tag{3.17}$$

Setting $w_N = \xi_v^{n+1/2}$in (3.11) and taking the real part, we obtain

$$\frac{\|\xi_v^{n+1}\|^2 - \|\xi_v^n\|^2}{2\tau} = \mathrm{Re}\Big\{(\mathcal{R}_2^{n+\frac{1}{2}}, \xi_v^{n+1/2}) - \mathcal{A}(\xi_u^{n+\frac{1}{2}}, \xi_v^{n+1/2}) - \frac{\beta}{2}\Big(\mathcal{N}^{n+1/2}, \xi_v^{n+1/2}\Big)\Big\}. \tag{3.18}$$

Taking into account of $\xi_u^n, \xi_v^n \in X_N^0$ and the definition of $\Pi_N^{\alpha/2,0}$, it holds

$$(\xi_v^{n+1/2} - \delta_t\xi_u^{n+1/2}, w_N) = (\Pi_N^{\alpha,0}\xi_v^{n+1/2} - \Pi_N^{\alpha,0}\delta_t\xi_u^{n+1/2}, w_N), \quad \forall w_N \in X_N^0(\Omega), \tag{3.19}$$

then we have

$$\begin{aligned}\mathcal{A}(\xi_u^{n+\frac{1}{2}}, \xi_v^{n+1/2}) &= \mathcal{A}(\xi_u^{n+\frac{1}{2}}, \delta_t\xi_u^{n+1/2}) - \mathcal{A}(\xi_u^{n+\frac{1}{2}}, \delta_t\xi_u^{n+1/2} - \xi_v^{n+1/2}) \\ &= \frac{|\xi_u^{n+1}|_{\alpha/2} - |\xi_u^n|_{\alpha/2}}{2\tau} - \mathcal{A}(\xi_u^{n+\frac{1}{2}}, \Pi_N^{\alpha/2,0}\delta_t\xi_u^{n+1/2} - \Pi_N^{\alpha/2,0}\xi_v^{n+1/2}),\end{aligned} \tag{3.20}$$

in which

$$\begin{aligned}&|\mathcal{A}(\xi_u^{n+\frac{1}{2}}, \Pi_N^{\alpha/2,0}\delta_t\xi_u^{n+1/2} - \Pi_N^{\alpha/2,0}\xi_v^{n+1/2})| \\ &\quad = |\mathcal{A}(\xi_u^{n+\frac{1}{2}}, \Pi_N^{\alpha/2,0}\delta_t\xi_u^{n+1/2} - \delta_t\xi_u^{n+1/2} + \delta_t\xi_u^{n+1/2} - \xi_v^{n+1/2} + \xi_v^{n+1/2} - \Pi_N^{\alpha/2,0}\xi_v^{n+1/2})| \\ &\quad \leq \mathcal{C}|\xi_u^{n+\frac{1}{2}}|_{\alpha/2}\Big(|\Pi_N^{\alpha/2,0}\delta_t\xi_u^{n+1/2} - \delta_t\xi_u^{n+1/2}|_{\alpha/2} + |\delta_t\xi_u^{n+1/2} - \xi_v^{n+1/2}|_{\alpha/2} + |\xi_v^{n+1/2} - \Pi_N^{\alpha/2,0}\xi_v^{n+1/2}|_{\alpha/2}\Big) \\ &\quad \leq \mathcal{C}\Big(|\xi_u^{n+1}|_{\alpha/2}^2 + |\xi_u^n|_{\alpha/2}^2 + \tau^4 + N^{\alpha-2r}\Big).\end{aligned}$$

Thus, we conclude

$$|\mathcal{A}(\xi_u^{n+\frac{1}{2}}, \xi_v^{n+1/2})| \leq \frac{|\xi_u^{n+1}|_{\alpha/2}^2 - |\xi_u^n|_{\alpha/2}^2}{2\tau} + \mathcal{C}\Big(|\xi_u^{n+1}|_{\alpha/2}^2 + |\xi_u^n|_{\alpha/2}^2 + \tau^4 + N^{\alpha-2r}\Big). \tag{3.21}$$

By using (3.15) and the Cauchy-Schwarz inequality, we have

$$|(\mathcal{R}_2^{n+\frac{1}{2}}, \xi_v^{n+1/2})| \leq \mathcal{C}\Big(\|\xi_v^{n+1}\|^2 + \|\xi_v^n\|^2 + \tau^4\Big), \tag{3.22}$$

and

$$|(\mathcal{N}^{n+1/2}, \xi_v^{n+1/2})| \leq \mathcal{C}\Big(\|\mathcal{N}^{n+1/2}\|^2 + \|\xi_v^{n+1}\|^2 + \|\xi_v^n\|^2\Big) \tag{3.23}$$

$$\leq \Big(\|\xi_u^{n+1}\|^2 + \|\xi_u^n\|^2 + \|\xi_v^{n+1}\|^2 + \|\xi_v^n\|^2 + N^{-2r}\Big), \tag{3.24}$$

Substituting (3.21)-(3.23) into (3.18), we obtain

$$|\xi_u^{n+1}|_{\alpha/2}^2 + \|\xi_v^{n+1}\|^2 \leq |\xi_u^n|_{\alpha/2}^2 + \|\xi_v^n\|^2$$

$$+\mathcal{C}\tau\Big(\|\xi_u^{n+1}\|^2+\|\xi_u^n\|^2+|\xi_u^{n+1}|_{\alpha/2}^2+|\xi_u^n|_{\alpha/2}^2+\|\xi_v^{n+1}\|^2+\|\xi_v^n\|^2+\tau^4+N^{-2r}\Big). \tag{3.25}$$

Summing up (3.17) and (3.25), we conclude that

$$H^{n+1}\le H^n+\mathcal{C}\tau\Big(H^{n+1}+H^n+\tau^4+N^{\alpha-2r}\Big),$$

where

$$H^n=\|\xi_u^n\|^2+|\xi_u^n|_{\alpha/2}^2+\|\xi_v^n\|^2.$$

According to the Grownwall inequality (Lemma 3.2), we obtain

$$H^n\le\mathcal{C}(\tau^4+N^{\alpha-2r}).$$

Thus, we have

$$\max_{1\le n\le N_t}\Big\{\|\xi_u^n\|,|\xi_u^n|_{\alpha/2},\|\xi_v^n\|\Big\}\le\mathcal{C}(\tau^2+N^{\alpha/2-r}).$$

By admitting Theorem 3.1, we derive

$$\|u^n-U_N^n\|\le\|u^n-\Pi_N^{\alpha/2,0}u^n\|+\|\xi_u^n\|\le\mathcal{C}(\tau^2+N^{\alpha/2-r}),$$

and

$$|u^n-U_N^n|_{\alpha/2}\le|u^n-\Pi_N^{\alpha/2,0}u^n|_{\alpha/2}+|\xi_u^n|_{\alpha/2}\le\mathcal{C}(\tau^2+N^{\alpha/2-r}).$$

Thanks to the Sobolev inequality (Theorem 3.3), we arrive at

$$\|u^n-U_N^n\|_\infty\le\mathcal{C}\sqrt{\|u^n-U_N^n\|+|u^n-U_N^n|_{\alpha/2}}\le\mathcal{C}(\tau^2+N^{\alpha/2-r}).$$

This completes the proof. □

Corollary 3.1. *Under the conditions of Theorem 3.4, the solution U_N^n at the time level n of the numerical scheme (3.4)-(3.5) is unconditionally stable with respect to initial values in L^2 and L^∞ norms.*

4 The energy quadratization SAV–GLS method

The SAV formulation of the FNLS equation (1.1) introduces a scalar auxiliary variable

$$p(t)=\sqrt{\int_\Omega\frac{1}{2}|u|^4dx+C_0}\quad\text{with}\quad F(u)=\frac{|u|^2}{\sqrt{\int_\Omega\frac{1}{2}|u|^4dx+C_0}},$$

with a positive C_0 (which guarantees that the function p has a positive lower bound), and reformulate (1.1) as

$$u_t=v\quad\text{in}\quad\Omega\times(0,T], \tag{4.1}$$
$$v_t+(-\Delta)^{\frac{\alpha}{2}}u+\mathrm{i}\kappa v+\beta pF(u)u=0\quad\text{in}\quad\Omega\times(0,T], \tag{4.2}$$
$$p_t=\mathrm{Re}(F(u)u,v)\quad\text{in}\quad\Omega\times(0,T], \tag{4.3}$$
$$u=0\qquad\text{on}\quad\partial\Omega\times(0,T], \tag{4.4}$$
$$u=u_0,\quad v=u_1,\quad p=p_0\quad\text{in}\quad\Omega\times\{0\}, \tag{4.5}$$

where $p_0 = \sqrt{\int_\Omega \frac{1}{2}|u_0|^4 dx + C_0}$. The energy conservation in the SAV formulation is

$$\frac{d}{dt}\Big(v^2 + |u|^2_{\alpha/2} + \beta p^2 - \beta C_0\Big) = 0.$$

By using the implicit midpoint method in time, and the spectral Galerkin method is applied in space for (4.1)-(4.3), the fully SAV–GLS scheme is constructed, i.e., finding $U_N^n, V_N^n \in X_N^0(\Omega)$, for $w_N \in X_N^0(\Omega)$, such that

$$(\delta_t U_N^{n+1/2}, w_N) = (V_N^{n+1/2}, w_N), \tag{4.6}$$

$$(\delta_t V_N^{n+1/2}, w_N) + \mathcal{A}(U_N^{n+1/2}, w_N) + \mathrm{i}\kappa(V_N^{n+1/2}, w_N) + \beta P^{n+1/2}(F(U_N^{n+1/2})U_N^{n+1/2}, w_N) = 0, \tag{4.7}$$

$$\delta_t P^{n+1/2} = \mathrm{Re}(F(U_N^{n+1/2})U_N^{n+1/2}, V_N^{n+1/2}). \tag{4.8}$$

Theorem 4.1 (**SAV–GLS: Conservative law**). *The numerical solution of the SAV-GLS scheme* (4.6)-(4.8) *is conservative in the sense that*

$$\mathcal{E}^{n+1} = \mathcal{E}^n = \cdots = \mathcal{E}^0,$$

with

$$\mathcal{E}^n = \|V_N^n\|^2 + |U_N^n|^2_{\alpha/2} + \beta(P^n)^2 - \beta C_0, \quad 0 \le n \le N_t.$$

Proof. Choosing $w_N = \delta_t U_N^{n+\frac{1}{2}}$ in (4.7), and taking the real part, the energy conservation is immediate. □

Theorem 4.2 (**SAV–GLS: Boundness**). *The numerical solution of the scheme* (4.6)-(4.8) *is long-time bounded in the following sense*

$$\|U_N^n\| \le \mathcal{C}, \quad \|U_N^n\|_\infty \le \mathcal{C}, \quad 0 \le n \le N_t.$$

Proof. In view of $\beta(P^n)^2 - \beta C_0 \ge 0$, the proof is same as Theorem 3.2. Here we omit the proof for brevity. □

Remark 4.1. *It is worth pointing out that there are some works focus on the linearly implicit SAV methods for the gradient flow system [37] and conservative system [7] by the extrapolation technique. We notice that the extrapolation technique could cause the implementation of SAV-GLS scheme become more complex. In the current paper, we just consider the implicit-midpoint SAV-GLS method with quadratic energy.*

5 The linearly implicit ESAV–GLS method

The ESAV formulation of the FNLS equation (1.1) introduces a exponential scalar auxiliary variable

$$q(t) = \exp\Big(\int_\Omega \frac{1}{2}|u|^4 dx\Big) \quad \text{with} \quad \mathcal{F}(u) = \frac{|u|^2}{\exp\Big(\int_\Omega \frac{1}{2}|u|^4 dx\Big)}.$$

The system (1.1) can be reformulated as

$$u_t = v \quad \text{in} \quad \Omega \times (0, T], \tag{5.1}$$

$$v_t + (-\Delta)^{\frac{\alpha}{2}} u + \mathrm{i}\kappa v + \beta q \mathcal{F}(u) u = 0 \quad \text{in} \quad \Omega \times (0, T], \tag{5.2}$$

$$\frac{d}{dt}\ln(q) = 2\mathrm{Re}(q\mathcal{F}(u)u, v) \quad \text{in} \quad \Omega \times (0, T], \tag{5.3}$$

$$u = 0 \qquad \text{on} \quad \partial\Omega \times (0, T], \tag{5.4}$$

$$u = u_0, \quad v = u_1, \quad q = q_0 \quad \text{in} \quad \Omega \times \{0\}, \tag{5.5}$$

where $q_0 = \exp\Big(\int_\Omega \frac{1}{2}|u_0|^4 dx\Big)$. The energy conservation in the ESAV formulation is

$$\frac{d}{dt}\Big(v^2 + |u|^2_{\alpha/2} + \beta \ln(q)\Big) = 0.$$

The fully ESAV–GLS scheme is constructed by combining the implicit midpoint method and spectral Galerkin method for (5.1)-(5.3), i.e., finding $U_N^n, V_N^n \in X_N^0(\Omega)$, for $w_N \in X_N^0(\Omega)$, such that

$$(\delta_t U_N^{n+1/2}, w_N) = (V_N^{n+1/2}, w_N), \tag{5.6}$$

$$(\delta_t V_N^{n+1/2}, w_N) + \mathcal{A}(U_N^{n+1/2}, w_N) + \mathrm{i}\kappa(V_N^{n+1/2}, w_N) + \beta\widetilde{Q}^{n+1/2}(F(\widetilde{U}_N^{n+1/2})\widetilde{U}_N^{n+1/2}, w_N) = 0, \tag{5.7}$$

$$\delta_t \ln(Q^{n+1/2}) = 2\widetilde{Q}^{n+1/2}\mathrm{Re}(F(\widetilde{U}_N^{n+1/2})\widetilde{U}_N^{n+1/2}, V_N^{n+1/2}), \tag{5.8}$$

with the initial-start scheme

$$(\delta_t U_N^{1/2}, w_N) = (V_N^{1/2}, w_N), \tag{5.9}$$

$$(\delta_t V_N^{1/2}, w_N) + \mathcal{A}(U_N^{1/2}, w_N) + \mathrm{i}\kappa(V_N^{1/2}, w_N) + \beta Q^{1/2}(F(U_N^{1/2})U_N^{1/2}, w_N) = 0, \tag{5.10}$$

$$\delta_t \ln(Q^{1/2}) = 2Q^{1/2}\mathrm{Re}(F(U_N^{1/2})U_N^{1/2}, V_N^{1/2}). \tag{5.11}$$

In a similar proof of SAV-GLS, we have the following conservation and boundness.

Theorem 5.1 (**ESAV–GLS: Conservative law**). *The numerical solution of the SAV–GLS scheme* (5.6)-(5.8) *is conservative in the sense that*

$$\mathcal{E}^{n+1} = \mathcal{E}^n = \cdots = \mathcal{E}^0,$$

with

$$\mathcal{E}^n = \|V_N^n\|^2 + |U_N^n|^2_{\alpha/2} + \beta \ln(Q^n), \quad 0 \le n \le N_t.$$

Theorem 5.2 (**ESAV–GLS: Boundness**). *The numerical solution of the scheme* (5.6)-(5.8) *is long-time bounded in the following sense*

$$\|U_N^n\| \le \mathcal{C}, \quad \|U_N^n\|_\infty \le \mathcal{C}, \quad 0 \le n \le N_t.$$

Remark 5.1. *By admitting the $L^\infty-$norm boundness of the numerical solutions of SAV–GLS method and ESAV–GLS method, it is easy to check that the nonlinear terms $F(u)$ and $\mathcal{F}(u)$ both satisfy the global Lipschitz conditions. This fact offers possibilities for the SAV–GLS method and ESAV–GLS method to discuss the unconditional convergence and stability in L^2 and L^∞ norms, respectively.*

6 Implementation

In this section, we take the CN–GLS method (3.4)-(3.5) as an example to illustrate the implementations. The approximation polynomial spaces $X_N^0(\Omega)$ can be expressed as

$$X_N^0(\Omega) = \mathrm{span}\{\phi_k(x): \ k = 0, 1, \cdots, N-2\},$$

in which $\phi_k(x)$ is determined by the following recurrence relation

$$\phi_k(x) = L_k(\widehat{x}) - L_{k+2}(\widehat{x}), \quad \widehat{x} \in [-1, 1], \quad x = \frac{(b-a)\widehat{x} + (a+b)}{2} \in [a, b],$$

where $L_k(\hat{x})$ is the Legendre polynomial which satisfies the three-term recurrence relation [36]

$$
\begin{aligned}
&L_0(\hat{x}) = 1, \quad L_1(\hat{x}) = \hat{x}, \\
&(k+1)L_{k+1}(\hat{x}) = (2k+1)\hat{x}L_k(\hat{x}) - kL_{k-1}(\hat{x}), \quad k \geq 1.
\end{aligned}
$$

Denote the numerical solutions U_N^n and V_N^n as

$$
U_N^n = \sum_{k=0}^{N-2} \widehat{U}_k^n \phi_k(x), \qquad V_N^n = \sum_{k=0}^{N-2} \widehat{V}_k^n \phi_k(x).
$$

Then we give the mass and stiff matrices of the CN–GLS scheme as follows

$$
M_{l,k}^x = (\phi_k(x), \phi_l(x)), \quad S_{l,k}^x = \frac{1}{2\cos(\frac{\alpha\pi}{2})}\Big[\Big({}_a^{RL}D_x^{\alpha/2}\phi_k(x), {}_x^{RL}D_b^{\alpha/2}\phi_l(x)\Big) + \Big({}_x^{RL}D_b^{\alpha/2}\phi_k(x), {}_a^{RL}D_x^{\alpha/2}\phi_l(x)\Big)\Big],
$$

where M^x, and S^x are all symmetric, the computations of the entries of the mass and stiff matrices can be found in [46]. The linearized iterative algorithm of CN–GLS scheme can be expressed as

$$
(M^x + \frac{\tau^2}{4}S^x + \frac{\mathrm{i}\kappa\tau}{2}M^x)\widehat{U}^{n+1,s+1} = (M^x - \frac{\tau^2}{4}S^x + \frac{\mathrm{i}\kappa\tau}{2}M^x)\widehat{U}^n + \tau M^x\widehat{V}^n - \frac{\beta\tau^2}{8}\mathcal{N}^{n+1,s}, \ s = 0, 1, 2, \cdots,
$$

with

$$
\widehat{U}^{n+1,0} = \begin{cases} \widehat{U}^0, & n = 0, \\ 2\widehat{U}^n - \widehat{U}^{n-1}, & n \geq 1, \end{cases}
$$

where $(\mathcal{N}^{n+1,s})_l = \Big((|U_N^n|^2 + |U_N^{n+1,s}|^2)(U_N^n + U_N^{n+1,s}), \phi_l\Big)$, $l = 0, 1, \cdots, N-2$. Then $U_N^{n+1,s}$ numerically converges to U_N^{n+1} if there satisfies $\|U_N^{n+1,s+1} - U_N^{n+1,s}\|_\infty \leq \epsilon$ for the given stopping criteria ϵ [2].

7 Numerical experiments

In this section, we intend to report the numerical results of the CN–GLS, SAV–GLS and ESAV–GLS methods by using Matlab R2018a software on a computer with Intel Core i7 and 16 GB RAM. Without special instructions, we always take the stopping criteria $\epsilon = 10^{-14}$ and the constant $C_0 = 1$.

Denote the L^2-norm error as

$$
\|u^{Nt} - U_N^{Nt}\| = \sqrt{\frac{b-a}{2}\sum_{j=0}^{M}\Big(u(x_j, T) - U_N^{N_t}(x_j)\Big)^2 w_j}, \quad \text{with} \quad x_j = \frac{(b-a)\widehat{x}_j + (a+b)}{2},
$$

where $\{\widehat{x}_j\}$ and $\{w_j\}$ are points and weights of the Legendre–Gauss–Lobatto quadrature [36], respectively, and $M = \mu N$ $(\mu > 1, \mu \in \mathbb{N}_+)$.

The L^∞-norm error is computed by

$$
\|u^{Nt} - U_N^{Nt}\|_\infty = \max_{0\leq j\leq M}\Big|u(x_j, T) - U_N^{N_t}(x_j)\Big|.
$$

The relative energy deviation is defined as

$$
\mathrm{RE}^n = \frac{|\mathcal{E}^n - \mathcal{E}^0|}{\mathcal{E}^0}.
$$

It is worth noting that, for the case which the exact solution is unknown, we compute the reference "exact" solutions with large $N = 600$ and $\tau = 10^{-5}$.

Table. 1: Abbreviations of the numerical schemes.

• **CN–GLS**:	The spectral Galerkin method (3.4)-(3.5) with an accuracy of $\mathcal{O}(\tau^2 + N^{\alpha/2-r})$.
• **SAV–GLS**:	The spectral Galerkin method (4.6)-(4.8) with an accuracy of $\mathcal{O}(\tau^2 + N^{\alpha/2-r})$.
• **ESAV–GLS**:	The spectral Galerkin method (5.6)-(5.8) with an accuracy of $\mathcal{O}(\tau^2 + N^{\alpha/2-r})$.
• **LF–FDM**:	The finite difference method [35] with an accuracy of $\mathcal{O}(\tau^2 + N^{-2})$.

Example 7.1 (**Numerical accuracy**)**.** Consider the following equation with a source term

$$u_{tt} + (-\Delta)^{\frac{\alpha}{2}} u + 2\mathrm{i}u_t + |u|^2 u = f(x,t), \quad (x,t) \in (0,1) \times (0,1]$$

The initial datum are determined by the exact solution

$$u(x,t) = \mathrm{i}\exp(-t)x^r(1-x)^r, \quad r \in \mathbb{N}_+.$$

The explicit expression of $f(x,t)$ can be found in Ref. [9].

For this linear example, we apply our proposed spectral Galerkin methods (CN–GLS method, SAV–GLS method and ESAV–GLS method) and the existing finite difference method to solve Ex. 7.1. For the fixed polynomial degree $N = 400$ and $r = 2$, the L^2- and L^∞-norm errors as well as the corresponding temporal convergence orders are listed in Tab. 2-Tab. 4. It is obvious to find that the comparing numerical schemes uniformly possess the second order accuracy in time direction. Taking the temporal step $\tau = 10^{-4}$ and various polynomial degrees N for $r = 2, 4, 6$, the numerical results are shown in Tab. 5–Tab. 7. The spatial observation orders confirm that the spectral accuracy could be observed for the sufficiently large r and small time step τ. Numerical results of Tab. 5-Tab. 7 also illustrate that the spectral methods enjoy the more superior numerical accuracy than finite difference method. In the other word, the spectral method can quickly reach the machine accuracy with a small N, but the difference method can not achieve.

Table. 2: Temporal accuracy of the numerical schemes for Ex. 7.1 with $N = 400$, $r = 2$ and $\alpha = 1.4$.

Schemes	Errors \ Steps	$\tau = \frac{1}{10}$	$\tau = \frac{1}{20}$	$\tau = \frac{1}{40}$	$\tau = \frac{1}{80}$
CN–GLS	$\Vert u^{Nt} - U_N^{Nt}\Vert$	5.0687e-05	1.2682e-05	3.1713e-06	7.9287e-07
	Conv.rate	-	1.9988	1.9997	1.9999
	$\Vert u^{Nt} - U_N^{Nt}\Vert_\infty$	6.9832e-05	1.7233e-05	4.2934e-06	1.0724e-06
	Conv.rate	-	2.0187	2.0050	2.0013
SAV–GLS	$\Vert u^{Nt} - U_N^{Nt}\Vert$	5.0655e-05	1.2674e-05	3.1693e-06	7.9237e-07
	Conv.rate	-	1.9988	1.9997	1.9999
	$\Vert u^{Nt} - U_N^{Nt}\Vert_\infty$	6.9793e-05	1.7224e-05	4.2909e-06	1.0718e-06
	Conv.rate	-	2.0187	2.0050	2.0013
ESAV–GLS	$\Vert u^{Nt} - U_N^{Nt}\Vert$	5.0512e-05	1.2633e-05	3.1581e-06	7.8947e-07
	Conv.rate	-	1.9995	2.0000	2.0001
	$\Vert u^{Nt} - U_N^{Nt}\Vert_\infty$	6.9599e-05	1.7171e-05	4.2771e-06	1.0682e-06
	Conv.rate	-	2.0191	2.0053	2.0014
LF–FDM [35]	$\Vert u^{Nt} - U_N^{Nt}\Vert$	6.9750e-05	1.9606e-05	5.2819e-06	1.4715e-06
	Conv.rate	-	1.8309	1.8922	1.8438
	$\Vert u^{Nt} - U_N^{Nt}\Vert_\infty$	1.0195e-04	2.7380e-05	7.1959e-06	2.0072e-06
	Conv.rate	-	1.8967	1.9279	1.8420

Table. 3: Temporal accuracy of the numerical schemes for Ex. 7.1 with $N = 400$, $r = 2$ and $\alpha = 1.6$.

Schemes	Errors \ Steps	$\tau = \frac{1}{10}$	$\tau = \frac{1}{20}$	$\tau = \frac{1}{40}$	$\tau = \frac{1}{80}$
CN–GLS	$\Vert u^{Nt} - U_N^{Nt}\Vert$	5.4240e-05	1.3554e-05	3.3877e-06	8.4689e-07
	Conv.rate	-	2.0007	2.0003	2.0001
	$\Vert u^{Nt} - U_N^{Nt}\Vert_\infty$	6.6599e-05	1.7028e-05	4.2651e-06	1.0653e-06
	Conv.rate	-	1.9676	1.9972	2.0013
SAV–GLS	$\Vert u^{Nt} - U_N^{Nt}\Vert$	5.4213e-05	1.3547e-05	3.3861e-06	8.4646e-07
	Conv.rate	-	2.0007	2.0003	2.0001
	$\Vert u^{Nt} - U_N^{Nt}\Vert_\infty$	6.6568e-05	1.7020e-05	4.2631e-06	1.0648e-06
	Conv.rate	-	1.9676	1.9973	2.0013
ESAV–GLS	$\Vert u^{Nt} - U_N^{Nt}\Vert$	5.4084e-05	1.3510e-05	3.3764e-06	8.4399e-07
	Conv.rate	-	2.0011	2.0005	2.0002
	$\Vert u^{Nt} - U_N^{Nt}\Vert_\infty$	6.6416e-05	1.6977e-05	4.2517e-06	1.0619e-06
	Conv.rate	-	1.9680	1.9975	2.0014
LF–FDM [35]	$\Vert u^{Nt} - U_N^{Nt}\Vert$	5.7982e-05	1.6326e-05	4.497e-06	1.3755e-06
	Conv.rate	-	1.8284	1.8601	1.7090
	$\Vert u^{Nt} - U_N^{Nt}\Vert_\infty$	8.6524e-05	2.2784e-05	5.8879e-06	1.8948e-06
	Conv.rate	-	1.9251	1.9522	1.6357

Table. 4: Temporal accuracy of the numerical schemes for Ex. 7.1 with $N = 400$, $r = 2$ and $\alpha = 1.8$.

Schemes	Errors \ Steps	$\tau = \frac{1}{10}$	$\tau = \frac{1}{20}$	$\tau = \frac{1}{40}$	$\tau = \frac{1}{80}$
CN–GLS	$\Vert u^{Nt} - U_N^{Nt}\Vert$	5.4681e-05	1.3581e-05	3.3901e-06	8.472e-07
	Conv.rate	-	2.0095	2.0022	2.0005
	$\Vert u^{Nt} - U_N^{Nt}\Vert_\infty$	7.2078e-05	1.9661e-05	4.9326e-06	1.2304e-06
	Conv.rate	-	1.8742	1.9949	2.0032
SAV–GLS	$\Vert u^{Nt} - U_N^{Nt}\Vert$	5.4660e-05	1.3575e-05	3.3888e-06	8.4688e-07
	Conv.rate	-	2.0095	2.0022	2.0005
	$\Vert u^{Nt} - U_N^{Nt}\Vert_\infty$	7.2051e-05	1.9654e-05	4.9308e-06	1.2300e-06
	Conv.rate	-	1.8742	1.9949	2.0032
ESAV–GLS	$\Vert u^{Nt} - U_N^{Nt}\Vert$	5.4554e-05	1.3547e-05	3.3814e-06	8.4502e-07
	Conv.rate	-	2.0097	2.0023	2.0006
	$\Vert u^{Nt} - U_N^{Nt}\Vert_\infty$	7.1916e-05	1.9616e-05	4.9208e-06	1.2274e-06
	Conv.rate	-	1.8743	1.9951	2.0033
LF–FDM [35]	$\Vert u^{Nt} - U_N^{Nt}\Vert$	4.6025e-05	1.2717e-05	3.6312e-06	1.3500e-06
	Conv.rate	-	1.8557	1.8083	1.4275
	$\Vert u^{Nt} - U_N^{Nt}\Vert_\infty$	5.9557e-05	1.6485e-05	5.0681e-06	2.0064e-06
	Conv.rate	-	1.8531	1.7016	1.3368

Table. 5: Spatial accuracy of the numerical schemes for Ex. 7.1 with $\tau = 10^{-4}$ and $r = 2$.

α	N	CN–GLS				LF–FDM [35]			
		$\|u^{Nt} - U_N^{Nt}\|$	Conv.rate	$\|u^{Nt} - U_N^{Nt}\|_\infty$	Conv.rate	$\|u^{Nt} - U_N^{Nt}\|$	Conv.rate	$\|u^{Nt} - U_N^{Nt}\|_\infty$	Conv.rate
1.4	2^3	7.8251e-07	-	1.4387e-06	-	1.0625e-03	-	1.5240e-03	-
	2^4	3.2646e-08	$N^{-4.5831}$	9.5681e-08	$N^{-3.9103}$	2.3044e-04	$N^{-2.2049}$	3.4017e-04	$N^{-2.1636}$
	2^5	8.8670e-10	$N^{-5.2023}$	2.9528e-09	$N^{-5.0181}$	5.0747e-05	$N^{-2.1830}$	7.7553e-05	$N^{-2.1330}$
	2^6	6.6681e-11	$N^{-3.7331}$	1.8638e-10	$N^{-3.9858}$	1.1409e-05	$N^{-2.1531}$	1.7949e-05	$N^{-2.1113}$
1.6	2^3	9.0825e-07	-	1.5756e-06	-	1.6408e-03	-	2.2045e-03	-
	2^4	4.5634e-08	$N^{-4.3149}$	9.5053e-08	$N^{-4.0510}$	3.7188e-04	$N^{-2.1415}$	4.6951e-04	$N^{-2.2312}$
	2^5	1.7700e-09	$N^{-4.6883}$	4.3493e-09	$N^{-4.4499}$	8.4706e-05	$N^{-2.1343}$	1.1534e-04	$N^{-2.0253}$
	2^6	4.0768e-11	$N^{-5.4402}$	2.5453e-10	$N^{-4.0949}$	1.9453e-05	$N^{-2.1225}$	2.8469e-05	$N^{-2.0184}$
1.8	2^3	8.8544e-07	-	1.1569e-06	-	2.3621e-03	-	3.2931e-03	-
	2^4	5.4509e-08	$N^{-4.0218}$	8.3552e-08	$N^{-3.7914}$	5.6108e-04	$N^{-2.0738}$	7.9435e-04	$N^{-2.0516}$
	2^5	2.5355e-09	$N^{-4.4261}$	4.7136e-09	$N^{-4.1478}$	1.3312e-04	$N^{-2.0755}$	1.9501e-04	$N^{-2.0262}$
	2^6	2.2045e-10	$N^{-3.5238}$	3.6016e-10	$N^{-3.7101}$	3.1589e-05	$N^{-2.0752}$	4.6206e-05	$N^{-2.0774}$

Table. 6: Spatial accuracy of the numerical schemes for Ex. 7.1 with $\tau = 10^{-4}$ and $r = 4$.

α	N	CN–GLS				LF–FDM [35]			
		$\|u^{Nt} - U_N^{Nt}\|$	Conv.rate	$\|u^{Nt} - U_N^{Nt}\|_\infty$	Conv.rate	$\|u^{Nt} - U_N^{Nt}\|$	Conv.rate	$\|u^{Nt} - U_N^{Nt}\|_\infty$	Conv.rate
1.4	2^3	2.6210e-10	-	5.2541e-10	-	3.4780e-05	-	5.3906e-05	-
	2^4	3.5097e-12	$N^{-6.2227}$	4.5208e-12	$N^{-6.8607}$	8.4337e-06	$N^{-2.0440}$	1.2631e-05	$N^{-2.0935}$
1.6	2^3	2.3398e-10	-	3.7366e-10	-	6.4787e-05	-	9.0932e-05	-
	2^4	1.2636e-12	$N^{-7.5327}$	2.1298e-12	$N^{-7.4549}$	1.5777e-05	$N^{-2.0379}$	2.4341e-05	$N^{-1.9014}$
1.8	2^3	2.0096e-10	-	2.6384e-10	-	3.4745e-05	-	4.8634e-05	-
	2^4	6.5536e-12	$N^{-4.9385}$	8.9557e-12	$N^{-4.8807}$	6.7183e-06	$N^{-2.3706}$	8.6281e-06	$N^{-2.4949}$

Table. 7: Spatial accuracy of the numerical schemes for Ex. 7.1 with $\tau = 10^{-4}$ and $r = 6$.

α	N	CN–GLS				LF–FDM [35]			
		$\|u^{Nt} - U_N^{Nt}\|$	Conv.rate	$\|u^{Nt} - U_N^{Nt}\|_\infty$	Conv.rate	$\|u^{Nt} - U_N^{Nt}\|$	Conv.rate	$\|u^{Nt} - U_N^{Nt}\|_\infty$	Conv.rate
1.4	2^3	6.0943e-07	-	8.6411e-07	-	3.4293e-06	-	5.1708e-06	-
	2^4	9.6911e-14	$N^{-22.5840}$	1.4380e-13	$N^{-22.5190}$	7.2950e-07	$N^{-2.2329}$	1.1791e-06	$N^{-2.1328}$
1.6	2^3	5.1591e-07	-	1.0640e-06	-	4.7316e-06	-	7.8430e-06	-
	2^4	1.4686e-13	$N^{-21.7440}$	2.2672e-13	$N^{-22.1620}$	1.3482e-06	$N^{-1.8113}$	2.4203e-06	$N^{-1.6962}$
1.8	2^3	4.8355e-07	-	7.1443e-07	-	4.1374e-06	-	6.8622e-06	-
	2^4	2.5897e-13	$N^{-20.8320}$	3.4652e-13	$N^{-20.9750}$	6.0925e-07	$N^{-2.7636}$	9.9311e-07	$N^{-2.7886}$

Example 7.2. We consider the FNLS equation (1.1) in domain $(-20, 20) \times (0, T]$, the initial datum are given as follows

$$u(x, 0) = (1 + \mathrm{i})x \exp\big(-10(1-x)^2\big), \quad u_t(x, 0) = 0, \quad x \in (-20, 20).$$

In this simulation, we carry out utilizing our proposed spectral methods for Ex. 7.2 with $\kappa = \beta = 1$. Taking the parameters $N = 400$, $\tau = 0.1$ and $T = 10$, the profiles of the numerical solutions of CN–GLS method are plotted in Fig. 1, which are in great agreement with the existing references [27, 35]. For the fixed polynomial degree $N = 400$, the CPU time costs of the CN–GLS method, SAV–GLS method and

ESAV–GLS method with various time steps τ ($\tau = 1/20, 1/40, 1/80, 1/160, 1/320$) at final time $T = 1$ are shown in Fig. 2. The numerical results verify that the linearly implicit ESAV–GLS method enjoys a more superior computation efficiency than the fully implicit CN–GLS method and SAV–GLS method, also, the CN–GLS method performs more effective than SAV–GLS method. For testing the conservative properties of the proposed numerical schemes, we apply the proposed spectral methods and the finite difference method to solve Ex. 7.2 with $N = 400$, $\tau = 0.1$ and $T = 100$ for comparisons, and the time evolution of relative energy deviations are plotted in Fig. 3. The relative energy errors uniform reach the machine accuracy verify that our proposed numerical schemes preserve the energy very well. This fact exactly confirms the correctness of Theorem 3.1, Theorem 4.1 and Theorem 5.1.

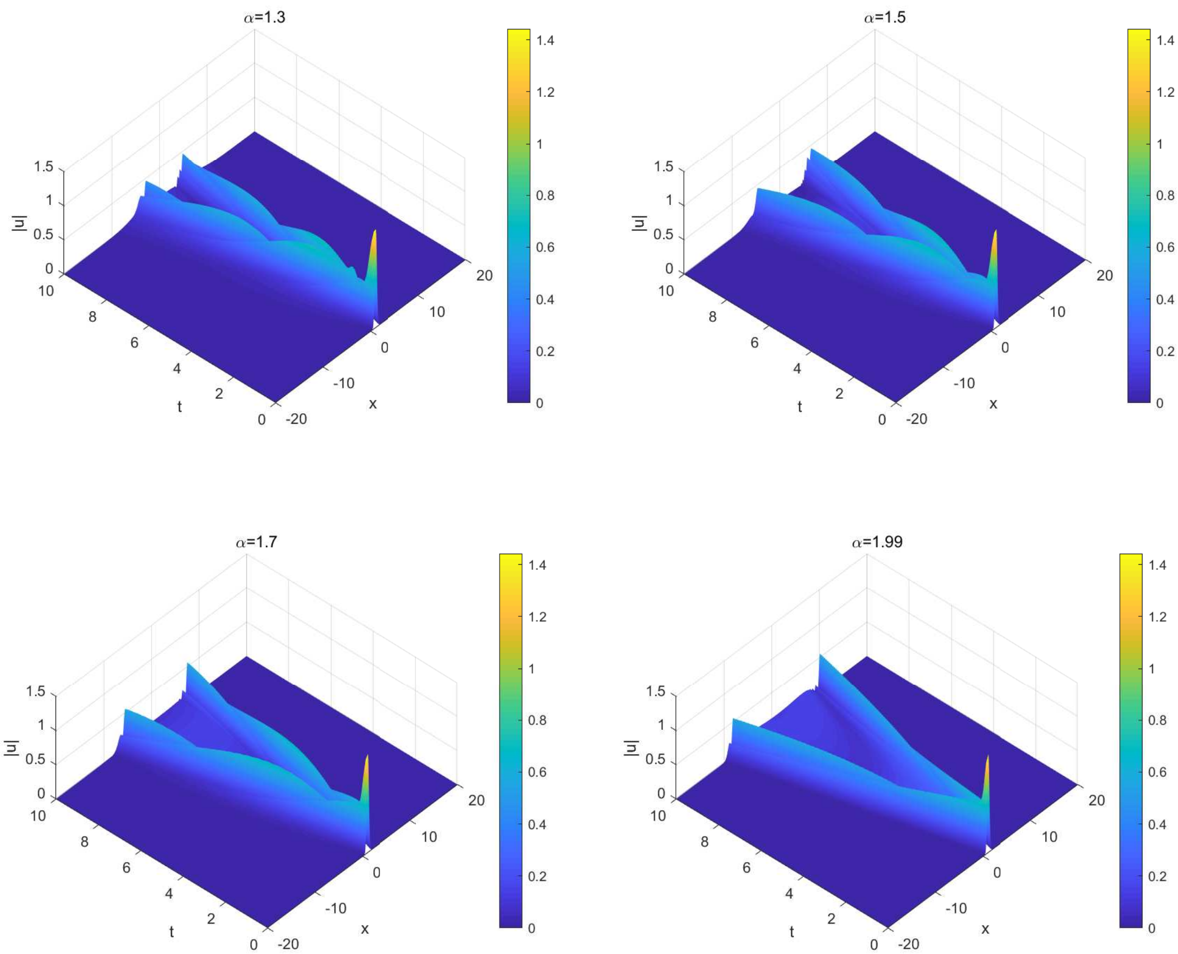

Fig. 1: Time evolution of numerical solutions for Ex. 7.2 with $N = 400$ and $\tau = 0.1$.

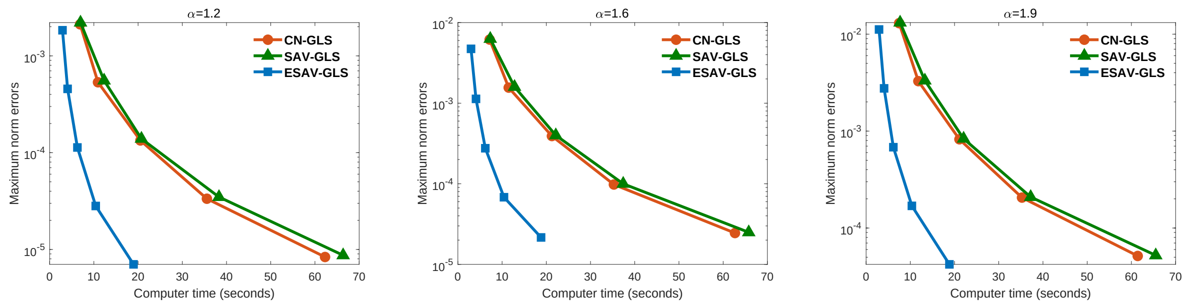

Fig. 2: Maximum norm errors and the corresponding CPU time costs for Ex. 7.2 with $N = 400$.

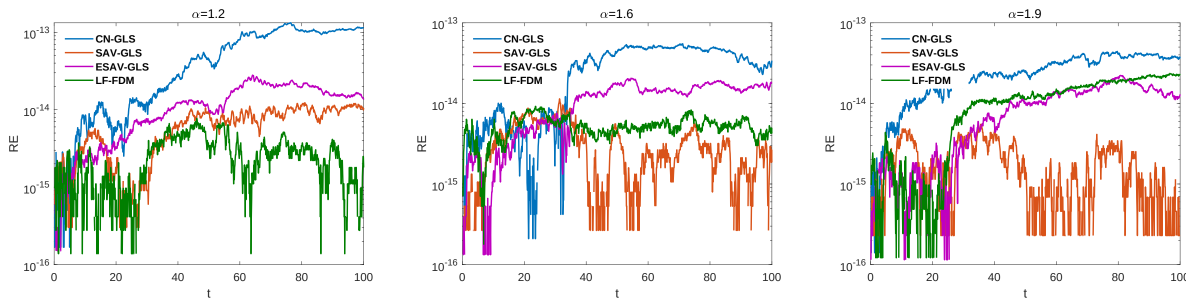

Fig. 3: Time evolution of the relative energy deviation for Ex. 7.2 with $N = 400$ and $\tau = 0.1$.

8 Conclusion

In this work, we have presented three Galerkin–Legendre spectral methods, involving the implicit CN–GLS method, the energy quadratization SAV–GLS method and the linearly implicit ESAV–GLS method, for solving the space-fractional nonlinear Schrödinger equation with wave operator. All the methods preserve the corresponding energy as continuous model. Moreover, we take the CN–GLS method as an example to illustrate that the proposed methods are unconditionally convergent and stable in L^∞ norm. Extensive numerical comparisons show that the theoretical analyses are correct. In recent years, there are some conservative schemes for the two–dimensional classical Schrödinger–type equations have also drawn much attention [15, 17, 30, 42]. In future study, we try to extend our proposed spectral Galerkin methods and the corresponding theoretical analyses to the two–dimensional fractional problems.

9 Acknowledgements

The authors would like to express the thanks to the referees for their valuable comments and suggestions. This work is supported by the National Key Research and Development Project of China (Grant No. 2018YFC1504205), the National Natural Science Foundation of China (Grant Nos. 11771213, 61872422, 11971242), the Key Project of Jiangsu University Natural Science Foundation (Grant No. 18KJA110003), the Postgraduate Research & Practice Innovation Program of Jiangsu Province (Grant No. KYCX20_1165), and the Priority Academic Program Development of Jiangsu Higher Education Institutions.

References

[1] Akrivis G., Dougalis V., Karakashian O., On fully discrete Galerkin methods of second-order temporal accuracy for the nonlinear Schrödinger equation, *Numer. Math.,* **59** (1991), 31-53.

[2] An J., Cao W., Zhang z., An efficient spectral Petrov-Galerkin method for nonlinear Hamiltonian systems, *Commun. Comput. Phys.,* **26** (2019), 1249-1273.

[3] Bao W., Cai Y., Uniform error estimates of finite difference methods for the nonlinear Schrödinger equation with wave operator, *SIAM J. Numer. Anal.,* **50** (2012), 492-521.

[4] Bu W., Tang Y., Wu Y., Yang J., Crank-Nicolson ADI Galerkin finite element method for two-dimensional fractional FitzHugh-Nagumo monodomain model, *Appl. Math. Comput.,* **257** (2015), 355-64.

[5] Brugnano L., Iavernaro F., Line integral methods for conservative problems, Chapman and Hall/CRC, Boca Raton, FL, 2016.

[6] Claudianor O., Marcelo M., On existence, uniform decay rates and blow up for solutions of the 2-D wave equation with exponential source, *Calc. Var. Partial Differ. Equs.,* **34** (2009), 377-411.

[7] Cai W., Jiang C., Wang Y., Song Y., Structure-preserving algorithms for the two-dimensional sine-Gordon equation with Neumann boundary conditions, *J. Comput. Phys.,* **395** (2019), 166-185.

[8] Cai W., He D., Pan K., A linearized energy-conservative finite element method for the nonlinear Schrödinger equation with wave operator *Appl. Numer. Math.,* **140** (2019), 183-198.

[9] Ding H., Li C., High-order algorithms for Riesz derivative and their applications (III), *Fract. Calc. Appl. Anal.,* **19** (2016), 19-55.

[10] Duo S., Zhang Y., Accurate numerical methods for two and three dimensional integral fractional Laplacian with applications, *Comput. Methods Appl. Mech. Engrg.*, **355** (2019) 639-662.

[11] Ervin V., Roop J., Variational formulation for the stationary fractional advection dispersion equation, *Numer. Methods for Partial Differential Equs.,* **22** (2006), 558-576.

[12] Furihata D., Matsuo T., Discrete Variational Derivative Method. A Structure-Preserving Numerical Method for Partial Differential Equations, Chapman Hall/CRC, Boca Raton, FL, 2011.

[13] Guo X., Xu M., Some physical applications of fractional Schrödinger equation, *J. Math. Phys.,* **47** (2006), 082.

[14] Guo B., Han Y., Xin J., Existence of the global smooth solution to the period boundary value problem of fractional nonlinear Schrödinger equation, *Appl. Math. Comput.,* **204** (2008), 468-477.

[15] Guo L., Xu Y., Energy Conserving local discontinuous Galerkin methods for the nonlinear Schrödinger equation with wave operator, *J. Sci. Comput.,* **65** (2015), 622-647.

[16] Gu X., Huang T., Ji C., Alikhanov A., Carpentieri B., Fast iterative method with a second-order implicit difference scheme for time-space fractional convection-diffusion equation, *J. Sci. Comput.,* **72** (2017), 957-985.

[17] Gong Y., Wang Q., Wang Y., Cai J., A conservative Fourier pseudo-spectral method for the nonlinear Schrödinger equation, *J. Comput. Phys.,* **328** (2017), 354-370.

[18] Hairer E., Lubich C., Wanner G., Geometric numerical integration: structure-preserving algorithms for ordinary differential equations, Springer-Verlag, Berlin, 2nd edition, 2006.

[19] Hu D., Cao X., A fourth-order compact ADI scheme for two-dimensional Riesz space fractional nonlinear reaction-diffusion equation, *Int. J. Comput. Math.,* **97** (2020), 1928-1948.

[20] Hu D., Cai W., Song Y., Wang Y., A fourth-order dissipation-preserving algorithm with fast implementation for space fractional nonlinear damped wave equations, *Commun. Nonlinear Sci. Numer. Simul.,* **91** (2020), 105432.

[21] Hu D., Cai W., Fu Y., Wang Y., Fast dissipation-preserving difference scheme for nonlinear generalized wave equations with the integral fractional Laplacian, *Commun. Nonlinear Sci. Numer. Simul.,* **99** (2021), 105786.

[22] Ionescu A., Pusateri F., Nonlinear fractional Schrödinger equations in one dimension, *J. Funct. Anal.,* **266** (2014), 139-176.

[23] Kirkpatrick K., Lenzmann E., Staffilani G., On the continuum limit for discrete NLS with long-range lattice interactions, *Comm. Math. Phys.,* **317** (2013), 563-591.

[24] Li S., Vu-Quoc L., Finite difference calculus invariant structure of a class of algorithms for the nonlinear Klein-Gordon equation, *SIAM J. Numer. Anal.,* **32** (1995), 1839-1875.

[25] Laskin N., Fractional quantum mechanics and Lévy path integrals, *Phys. Lett.,* **268** (2000), 298-305.

[26] Longhi S., Fractional Schrödinger equation in optics, *Opt. Lett.,* **40** (2015), 1117-1120.

[27] Li M., Zhao Y., A fast energy conserving finite element method for the nonlinear fractional Schrödinger equation with wave operator, *Appl. Math. Comput.,* **338** (2018), 758-773.

[28] Liu Z., Li X., The exponential scalar auxiliary variable (E-SAV) approach for phase field models and its explicit computing, *SIAM J. Sci. Comput.,* **42** (2020), B630-B655.

[29] Lischkea A., Panga G., Guliana M., Song F., Glusab C., Zheng X., Mao Z., Cai W., Meerschaert M., Ainsworth M., Karniadakis G., What is the fractional Laplacian? A comparative review with new results, *J. Comput. Phys.,* **404** (2020), 109009.

[30] Li S., Wang T., Wang J., Guo B., An efficient and accurate Fourier pseudo-spectral method for the nonlinear Schrödinger equation with wave operator, *Int. J. Comput. Math.,* **98** (2021), 340-356.

[31] Macías-Díaz J., Hendy A., De Staelen R., A pseudo energy-invariant method for relativistic wave equations with Riesz space-fractional derivatives, *Comput. Phy. Commun.,* **224** (2018), 98-107.

[32] Quispel G., McLaren D., A new class of energy-preserving numerical integration methods, *J. Phys. A: Math. Theor.,* **41** (2008), 045206.

[33] Podlubny I., Fractional differential equations, Academic Press, New York, 1999.

[34] Pan K., Zeng J., He D., Zhang S., A fourth-order difference scheme for the fractional nonlinear Schrödinger equation with wave operator, *Appl. Anal.,* (2020), doi: 10.1080/00036811.2020.1829600.

[35] Ran M., Zhang C., A linearly implicit conservative scheme for the fractional nonlinear Schrödinger equation with wave operator, *Int. J. Comput. Math.,* **93** (2016), 1103-1118.

[36] Shen J., Tang T., Wang L., Spectral methods: algorithms, analysis and applications, Springer Ser. Comput. Math., Springer, Heidelberg, 2011.

[37] Shen J., Xu J., Yang J., The scalar auxiliary variable (SAV) approach for gradient flows, *J. Comput. Phys.,* **353** (2018), 407-416.

[38] Sheng C., Shen J., Tang T., Wang L., Yuan H., Fast Fourier-like mapped Chebyshev spectral-Galerkin Methods for PDEs with integral fractional Laplacian in unbounded domains, *SIAM J. Numer. Anal.,* **58** (2020), 2435-2464.

[39] Tian W., Zhou H., Deng W., A class of second order difference approximations for solving space fractional diffusion equations, *Math. Comput.,* **84** (2015), 1703-1727.

[40] Wang P., Huang C., Zhao L., Point-wise error estimate of a conservative difference scheme for the fractional Schrödinger equation, *J. Comput. Appl. Math.,* **306** (2016), 231-247.

[41] Ying B., Liu Y., Li H., He S., Fast algorithm based on TT-M FE system for space fractional Allen-Cahn equations with smooth and non-smooth solutions, *J. Comput. Phys.,* **379** (2019), 351-372.

[42] Yang Y., Li H., Guo X., A linearized energy-conservative scheme for two-dimensional nonlinear Schrödinger equation with wave operator, *Appl. Math. Comput.,* **404** (2021), 126234.

[43] Zabusky N., Kruskal M., Interaction of "solitons" in a collisionless plasma and the recurrence of initial states, *Phys. Rev. Lett.,* **15** (1965), 240-243.

[44] Zhou Y., Application of discrete functional analysis to the finite difierence methods, International Academic Publishers, Beijing, 1990.

[45] Zhao X., Sun Z., Hao Z., A fourth-order compact ADI scheme for two-dimensional nonlinear space fractional Schrödinger equation, *SIAM J. Sci. Comput.,* **36** (2014), A2865-A2886.

[46] Zeng F., Liu F., Li C., Burrage K., Turner I., Anh V., A Crank-Nicolson ADI spectral method for a two-dimensional Riesz space fractional nonlinear reaction-diffusion equation, *SIAM J. Numer. Anal.,* **52** (2014), 2599-2622.

[47] Zhang L., Li C., Zhong H., Xu C., Lei D., Li Y., Fan D.. Propagation dynamics of super-Gaussian beams in fractional Schrödinger equation: from linear to nonlinear regimes, *Opt. Express.,* **24** (2016), 14406-14418.